Volume 9, Number 6
1009-1963/2000/09(06)/0469-05
CHINESE PHYSICS
June, 2000
© 2000 Chin. Phys. Soc.

# FERRIMAGNETIC PHASES OF THE BLUME-EMERY-GRIFFITHS MODEL AND THE POTTS MODEL ON THE DIAMOND LATTICE*

Ni Jun(倪 军) and Gu Bing-lin(顾秉林)

*Department of Physics, Tsinghua University, Beijing* 100084, *China*

(Received 3 June 1999; revised manuscript received 24 January 2000)

The phase transitions in the Blume-Emery-Griffiths (BEG) model and antiferromagnetic Potts model on the diamond lattice are investigated using the cluster-variation method in the pair approximation. The ferrimagnetic phases are found to be different from those on the simple-cubic lattice. The phase diagrams of the BEG model are also calculated. In the vicinity of the parameter line where the BEG model reduces to the three-state antiferromagnetic Potts model, new types of phase diagram are obtained. The results are different from those of the mean-field theory, which is a good approximation only for large coordination number of the lattice.

**PACC:** 7510H; 0550; 6460

## I. INTRODUCTION

The Blume-Emery-Griffiths(BEG) model[1] is a spin-1 model with bilinear and biquadratic nearest-neighbor pair interactions and a site potential. The model with vanishing biquadratic interaction is called the Blume-Capel model.[2] The spin-1 BEG model was originally introduced to describe phase separation and superfluid ordering in $^3$He–$^4$He mixture.[1] It has been applied to various systems, such as multicomponent fluids and multicomponent liquid crystal,[3] solid-liquid-gas system,[3] microemulsions,[4] semiconductor alloys,[5,6] and electronic conduction models.[7]

The Hamiltonian of the BEG model has the form

$$\mathcal{H} = J\sum_{\{i,j\}} s_i s_j - K\sum_{\{i,j\}} s_i^2 s_j^2 + \Delta\sum_i s_i^2, \qquad (1)$$

where $s_i = 0, \pm 1$ and $\{i,j\}$ indicates a sum over the nearest-neighbors. The BEG model exhibits a wide variety of transitions of first and second order. A very rich phase diagram was obtained for the bipartite lattice by means of mean field approximation (MFA),[1,8–10] renormalization-group (RG) techniques,[11–13] and Monte-Carlo (M-C) calculation.[14–17] The cluster-variation method (CVM) has also been used to reveal the rich structures in phase diagrams of the BEG model on a simple cubic lattice.[18] The MFA[10] found that there is a ferrimagnetic phase located between the ferromagnetic(F) and antiquadrupolar(A) phases in the phase diagram for $K/J < -1$. The M-C calculations[17] also exhibited the appearance of the ferrimagnetic phase in the BEG model on the simple-cubic (sc) lattice. Recently various approaches[18–23] have been used to investigate the region of the ferrimagnetic phase. In particular, the phase diagram of BEG model for $K/J = -3$, which is related to the three-state antiferromagnetic Potts model, is studied. Akheyan and Ananikian[23] investigated the BEG model on the Bethe lattice with the coordination number $z = 4$ and found that the type of the ferrimagnetic phase is different from that obtained by the MFA and also that of the sc lattice. For the ternary semiconductor alloys such as $(A^{\mathrm{III}}B^{\mathrm{V}})_{1-x}C^{\mathrm{IV}}_{2x}$,[5,6] if the three components of a discrete spin-1 variable are associated with each type of atoms: $s = 1 + (A^{\mathrm{III}}), 0(C^{\mathrm{IV}})$, and $-1(B^{\mathrm{V}})$, the phase transition of the system can be modeled by the BEG model on the diamond lattice with coordination $z = 4$.

In this paper, we will investigate ferrimagnetic phases of the BEG model and the related Potts model on the diamond lattice. We calculate the phase diagrams of the BEG model for the diamond lattice, which has the lowest coordination number among three-dimensional lattices. We will show that the results on the diamond lattice show significant differences between the MFA and the CVM results on the sc lattice.

## II. THE METHOD

The Hamiltonian of the three-component BEG spin model (Eq.(1)) is equivalent to the alloy Hamiltonian of a ternary system[1,2]

$$\mathcal{H} = \sum_{\{ij\}}\sum_{ss'} E_{ss'} c_i^s c_j^{s'} - N\sum_s \mu_s x_s, \qquad (2)$$

through mapping of the spin $s_i = \{+1, -1, 0\}$ onto the three species $A, B$, and $C$ of the ternary system. The variable $c_i^s = 1$ if the site $i$ is occupied by an

* Project supported by the National Natural Science Foundation of China (Grant No. 19804007).

$s(=A,B,C)$ atom and is zero otherwise. The notation $\{ij\}$ means summation over the pairs of nearest-neighbor lattice sites. $E_{ss'}$ represents the nearest-neighbor interaction energy. $N$ is the number of the lattice sites, $\mu_s$ is the chemical potential and $x_s$ is the concentration of the $s$ species. In the following, we will use subscript 1,2,3 to represent the $A, B, C$ species of the ternary system, respectively.

The energy parameters of the BEG Hamiltonian are related to the atomic nearest-neighbor interaction energies in the alloy Hamiltonian by the following equations:[2]

$$4J = E_{11} + E_{22} - 2E_{12}, \tag{3}$$

$$4K = -E_{11} - E_{22} - 2E_{12} - 4E_{33} + 4(E_{13} + E_{23}), \tag{4}$$

$$\Delta = \mu_3 - \frac{1}{2}(\mu_1 + \mu_2) - zE_{33} + \frac{z}{2}(E_{13} + E_{23}), \tag{5}$$

where $z$ is the coordination number of the lattice. Since there are no terms of $\sum s_i s_j^2$ and $\sum s_i^2 s_j$ in the BEG model, Eq.(1), with the up-down symmetry, we will use the symmetric alloy energy parameters between the species $A$ and $B$. In the following, we limit ourselves to the $J > 0$ case. The $J < 0$ case can be mapped on the $J > 0$ case by redefining the spin direction for one sublattice.

The BEG model for $K/J = -3$ and $\Delta/J = 2z$ with $J < 0$ corresponds to the three-state antiferromagnetic Potts model with the Hamiltonian

$$H = -2J \sum_{ij} \delta_{\sigma_i \sigma_j}, \tag{6}$$

where $\sigma_i = 1, 2, 3$ numbers the Potts states, and $\delta_{\sigma_i \sigma_j}$ is the Kronecker delta function.

The phase diagrams are calculated by the cluster-variation method[24,25] in the pair approximation, which is also often called the Bethe-Peierls approximation. In the pair approximation for the alloy Hamiltonian, the oriented-pair probability of the two-sublattice that an $s$ atom on an $\alpha$ sublattice site is bonded to an $s'$ atom on a $\beta$ sublattice site is represented by $P_{ss'}$ and the probability that an $s$ atom occupies an $\alpha$ sublattice site is represented by $P_s^\alpha$.

In the oriented-pair probability notation, the equilibrium state of the system is derived by minimizing the grand-canonical potential $G$ defined as

$$G = E - TS - \sum_{i=1}^{3} \mu_i N_i, \tag{7}$$

where $\mu_i$ is the chemical potential of the three species of atoms in the ternary system. $T$ is the absolute temperature. $E$ is the energy of the system given by

$$E = zN \sum_{i,j} E_{ij} P_{ij}, \tag{8}$$

where $N$ is the number of sites in the sublattice. $S$ is the configurational entropy given by

$$S = Nk_{\mathrm{B}} \left[ -z \sum_{i,j} P_{ij} \ln P_{ij} + (z-1) \sum_{i,\alpha} P_i^\alpha \ln P_i^\alpha \right], \tag{9}$$

where $k_{\mathrm{B}}$ is the Boltzmann's constant.

The symmetry of phase in the system is determined by the site probability $P_s^\alpha$. We can also describe the two-sublattice phase by the magnetization and quadrupolar moments of the sublattices $\alpha$ and $\beta$ in the BEG model.

$$\begin{aligned} m_\alpha &= < s_i >_\alpha, \quad m_\beta = < s_i >_\beta, \\ q_\alpha &= < s_i^2 >_\alpha, \quad q_\beta = < s_i^2 >_\beta . \end{aligned} \tag{10}$$

The values of these parameters define the following phases with different symmetry: 1) The disordered phase (D): $m_\alpha = m_\beta, q_\alpha = q_\beta$. 2) The ferromagnetic phase (F): $m_a = m_b \neq 0, q_\alpha = q_\beta$. 3) The antiquadrupolar phase (A): $m_\alpha = m_\beta = 0, q_\alpha \neq q_\beta$. 4) The ferrimagnetic phase (I): $m_\alpha \neq m_\beta \neq 0, q_\alpha \neq q_\beta$.

## Ⅲ. PHASE DIAGRAMS

The phase diagrams of the BEG model are calculated in the pair approximation. For the determination of the phase diagram of the system, we minimize the grand potential $G$ in which the chemical potentials $\Delta$ and temperature $T$ are the input variables. As we change the chemical potential and temperature $T$, we can determine the phase boundaries by searching for those special values of the chemical potentials $\Delta$ at which two phases coexist. First-order phase transition lines are determined by comparing the free energies of the different phases, and the second-order phase transition is determined from the vanishing of order parameters.

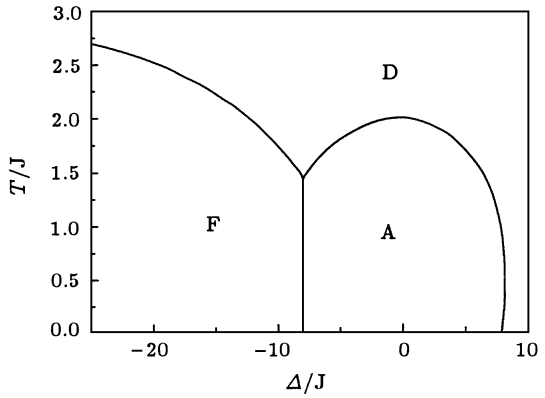



**Fig.1.** Phase diagram of the BEG model on the diamond lattice at $K/J = -3$. Disordered (D), ferromagnetic (F), and antiquadrupolar (A) phases are indicated. The enlarged part of the phase diagram along the line $\Delta/J = -8$ is shown in Fig.2.

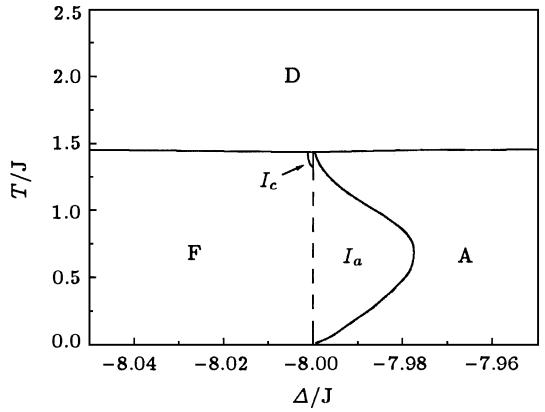



**Fig.2.** The ferrimagnetic phase regions in the phase diagram of the BEG model on the diamond lattice at $K/J = -3$. The dashed and solid lines indicate first and second-order phase transitions, respectively. Disordered (D), ferromagnetic (F), antiquadrupolar (A) and ferrimagnetic ($I_a$ and $I_c$) phases are indicated.

Figure 1 shows the phase diagram of the BEG model on the diamond lattice for $K/J = -3$. Since our CVM results give a much more narrow region of existence for the low-temperature ferrimagnetic phase ($-7.978 < \Delta/J < -8.002$), which is difficult to be distinguished on the scale of Fig.1, we show the enlarged part of the ferrimagnetic phase region close to the line $\Delta/J = -8$ in Fig.2. There are following differences between our results and those obtained by the MFA.[10] The type of the low-temperature ferrimagnetic phase is different from that of the MFA. The low-temperature ferrimagnetic phase for the diamond lattice is the ordered phase $I_a$ which is caused by the instability of the antiquadrupolar phase against spontaneous magnetization, while the low-temperature ferrimagnetic phase from the MFA is the ordered phase $I_b$ which is a result of instability of the ferromagnetic phase against the two-sublattice ordering. The low-temperature ferrimagnetic phase in Fig.2 is on the right side of the line $\Delta = -8$, while the low-temperature ferrimagnetic phase from the MFA is on the left side of the line $\Delta = -8$. So $\Delta = -8$ is a line of first-order transition. And the phase transition between the low-temperature ferrimagnetic phase and the ferromagnetic phase for the diamond lattice is of first order, and the phase transition between the ferrimagnetic phase and the antiquadrupolar phase is of second order. The MFA results predict a second-order transition between the ferromagnetic phase and the ferrimagnetic phase and first-order transition between the ferrimagnetic phase and the antiquadrupolar phase. Our result on the ferrimagnetic phase $I_a$ is similar to that of Akheyan and Ananikian.[23] The result is also different from that on the sc lattice.[18] For the sc lattice, the low-temperature ferrimagnetic phase is the phase $I_b$ which is the same as that of the MFA and is on the left side of the first-order transition line $\Delta = -8$. Reference [22] also found that the free energy of the ordered phase $I_a$ is smaller than that of the ordered phase $I_b$ on the diamond lattice. The results of Akheyan and Ananikian did not predict an intermediate ordered phase. We find an intermediate-temperature phase $I_c$ which is different from the intermediate ordered phase in the sc lattice.[18] The intermediate ordered phase in the sc lattice has a symmetry similar to the low-temperature ferrimagnetic phase $I_a$ in the diamond lattice. The intermediate-temperature ferrimagnetic phase $I_c$ is on the left side of the first-order transition line $\Delta/J = -8$ and the transition from the ferromagnetic phase to the ferrimagnetic phase $I_c$ is of second order. The other parts of the phase diagram of the BEG model on the diamond lattice for $K/J = -3$ in Fig.1 are similar to the MFA results. There occurs the reentrance near $\Delta = 0$ which has only a slight quantitative difference from the MFA results. Our CVM results give a more narrow region of reentrance. We have also calculated the corresponding phase diagram in temperature versus density $< s_i^2 >$, as shown in Fig.3, from which we can see that there is a coexistence region of the ferromagnetic phase and the ferrimagnetic phase $I_a$. At the intermediate temperature, the phase transition from the ferrimagnetic phase $I_c$ to the ferromagnetic phase is of second order, and there is a coexistence region of the ferrimagnetic phase $I_c$ and the ferrimagnetic phase $I_a$.

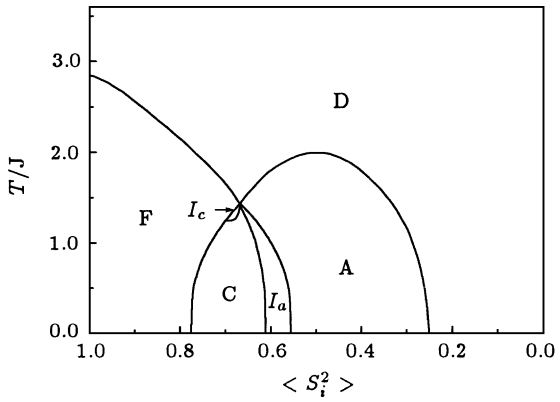



**Fig.3.** Phase diagram in temperature and density corresponding to Fig.1. Disordered (D), ferromagnetic (F), antiquadrupolar (A) and ferrimagnetic ($I_a$ and $I_c$) phases are indicated. C denotes the coexistence regions of the phases on each side.

We have also analyzed the phase transitions of the three-state antiferromagnetic Potts model, which is related to the appearance of the ferrimagnetic phases $I_a$ and $I_c$. In the phase diagram of the BEG model for $K/J = -3$, the line $\Delta/J = -2z$ corresponds to the three-state antiferromagnetic Potts model. Thus, the ordered phases of the antiferromagnetic Potts model for the diamond lattice correspond to the coexistent phases along the line $\Delta/J = -8$. On the line $\Delta/J = -8$, there are two phase transitions with the variation of the temperature. As a result, we found two ordered phases for the three-state antferrimagnetic Potts model. At temperatures below $T/J = 1.305$ the ordered phase is the phase $O_1$, in which one component has equal distribution in both sublattices and the other two components have an antiferromagnetic ordering. This is different from the low-temperature ordered phase $O_2$ which is found to occur in the sc ($z = 6$) lattice by the CVM and the MC method. In the ordered phase $O_2$, two of the components have the same distribution and the ordering occurs between these two components and the third component. The phase $O_2$ is the so-called broken-sublattice-symmetry (BSS) phase. In the MFA, in which the short range order is neglected and the entropy term is proportional to the coordination number of the lattice, the low-temperature ordered phase is the phase $O_2$ for all types of the lattice. From our calculation, it can be seen that with the decrease of the coordination number of the lattice $z$, the low-temperature ordered phase will change from the phase $O_2$ for the sc lattice with $z = 6$ to the phase $O_1$ for the diamond lattice with $z = 4$.

We also found an intermediate ordered phase $O_3$ on the diamond lattice which is different from both the ordered phases $O_1$ and $O_2$. The ordered phase $O_3$ at $1.305 < T/J < 1.438$ is 12 times degenerate, which is due to the sixfold permutational symmetry of the Potts states and the twofold symmetry of the sublattices. The transition from the disordered phase to the ordered phase $O_3$ is at the temperature $T/J = 1.438$. In the low-temperature region, the ordered phase $O_1$ with the sixfold degeneracy is related to the coexistence of the fourfold degenerate ferrimagnetic phase $I_a$ and the twofold degenerate ferromagnetic phases of the BEG model. At higher temepratures, the ordered phase $O_3$ corresponds to the coexistence of the ferrimagnetic phase $I_a$ and the ferrimagnetic phase $I_c$. The BEG model is a model with three components, but there is only one site potential $\Delta$ (or one chemical potential) in Eq.(1). If we consider another site potential, the ordered phase $O_3$ with 12 times degeneracy actually correponds to the coexistence of three fourfold degenerate ferrimagnetic phases in the Gibbs composition triangle.

## IV. CONCLUSIONS

In summary, we have investigated the phase transitions of the spin-1 BEG model on the diamond lattice. We determined the low-temperature ordered phases and calculated the phase diagrams with parameter $K/J = -3$. The ferrimagnetic phases for the diamond lattice are found to be different from those for the sc lattice. The topologies of the phase diagram is different from the MFA result and that for the sc lattice. The low-temperature ferrimagnetic phase for the diamond lattice is on the right side of the first-order transition line $\Delta/J = 2z$ and the intermediate-temperature ferrimagnetic phase is on the left side. The corresponding phase transitions of the three-state antiferromagnetic Potts model is also analyzed. There are two ordered phases for the three-state antiferromagnetic Potts model. The low-temperature ordered phase is the sixfold degenerate ordered phase $O_1$, which is related to the coexistence of the fourfold degenerate ferrimagnetic phase $I_a$ and the twofold degenerate ferromagnetic phases of the BEG model. The intermediate-temperature ordered phase is the ordered phase $O_3$ with 12 times degeneracy, corresponding to the coexistence of the ferrimagnetic phases of the BEG model.

## REFERENCES


[1] M. Blume, V. J. Emery, R. B. Griffiths, *Phys. Rev.*, **A4**(1971), 1071.

[2] D. Mukamel, M. Blume, *Phys. Rev.*, **A10**(1974), 610.

[3] J. Lajzerowicz, J. Sivardière, *Phys. Rev.*, **A11**(1975), 2079.

[4] M. Schick, W. H. Shih, *Phys. Rev.*, **B34**(1986), 1797.

[5] K. E. Newmann, J. D. Dow, *Phys. Rev.*, **B27**(1983), 7495.

[6] B. L. Gu, J. Ni, J. L. Zhu, *Phys. Rev.*, **B45**(1992), 4071.

[7] S. A. Kivelson, V. J. Emery, H. Q. Lin, *Phys. Rev.*, **B42**(1990), 6523.

[8] D. Furman, S. Dattagupta, R. B. Griffiths, *Phys. Rev.*, **B15**(1977), 441.

[9] V. Talanquer, C. Varea, A. Robledo, *Phys. Rev.*, **B39**(1989), 7030.

[10] W. Hoston, A. N. Berker, *Phys. Rev. Lett.*, **67**(1991), 1027.

[11] A. N. Berker, M. Wortis, *Phys. Rev.*, **B14**(1976), 4946.

[12] M. Kaufman, R. B. Griffiths, J. M. Yeomans, M. E. Fisher, *Phys. Rev.*, **B23**(1981), 3448.

[13] R. R. Netz, A. N. Berker, *Phys. Rev.*, **B47**(1993), 15019.

[14] M. Tanaka, T. Kawabe, *J. Phys. Soc. Jpn.*, **54**(1985), 2194.

[15] Y. L. Wang, C. Wentworth, *J. Appl. Phys.*, **61**(1987), 4411.

[16] Y. L. Wang, F. Lee, J. D. Kimel, *Phys. Rev.*, **B36**(1987), 8945.

[17] R. R. Netz, *Europhys. Lett.*, **17**(1992), 373.

[18] A. Rosengren, S. Lapinskas, *Phys. Rev. Lett.*, **71**(1993), 165.

[19] P. J. Kundrotas, S. Lapinskas, A. Rosengren, *Phys. Rev.*, **B52**(1995), 9166.

[20] A. Pelizzola, *Phys. Rev.*, **E54**(1996), R5885.

[21] R. K. Heilmann, J. S. Wang, R. H. Swendsen, *Phys. Rev.*, **B53**(1996), 2210.

[22] S. Lapinskas, A. Rosengren, *Phys. Rev. Lett.*, **81**(1998), 1302.

[23] A. Z. Akheyan, N. S. Ananikian, *J. Phys.*, **A29**(1996), 721.

[24] R. Kikuchi, *Phys. Rev.*, **81**(1951), 988.

[25] R. Kikuchi, *Acta Metall.*, **25**(1977), 195.